Magnetic configurations in nanostructured Co_2MnGa thin film elements

2015 New J. Phys. 17 083030

(http://iopscience.iop.org/1367-2630/17/8/083030)

New Journal of Physics
The open access journal at the forefront of physics

Deutsche Physikalische Gesellschaft DPG
IOP Institute of Physics

Published in partnership with: Deutsche Physikalische Gesellschaft and the Institute of Physics

OPEN ACCESS

RECEIVED
31 March 2015

REVISED
22 June 2015

ACCEPTED FOR PUBLICATION
13 July 2015

PUBLISHED
17 August 2015

PAPER

Magnetic configurations in nanostructured Co_2MnGa thin film elements

S Finizio[1], A Kronenberg[1], M Vafaee[1], M Foerster[2], K Litzius[1], A de Lucia[1], T O Menteş[3], L Aballe[2], B Krüger[1], M Jourdan[1] and M Kläui[1]

[1] Institut für Physik, Johannes Gutenberg Universität, Staudingerweg 7, D-55128 Mainz, Germany
[2] ALBA Synchrotron Light Source, Carretera BP 1413, km. 3.3, 08290 Cerdanyola del Valles, Spain
[3] Elettra Sincrotrone Trieste, I-34149 Basovizza (TS), Italy

E-mail: klaeui@uni-mainz.de

Keywords: Heusler compound, nanostructuring, x-ray microscopy

Abstract

The magnetic configuration of nanostructured elements fabricated from thin films of the Heusler compound Co_2MnGa was determined by high-resolution x-ray magnetic microscopy, and the magnetic properties of continuous Co_2MnGa thin films were determined by magnetometry measurements. A four-fold magnetic anisotropy with an anisotropy constant of $K_1 \approx 1.5$ kJ m^{-3} was deduced, and x-ray microscopy measurements have shown that the nanostructured Co_2MnGa elements exhibit reproducible magnetic states dominated by shape anisotropy, with a minor contribution from the magneto-crystalline anisotropy, showing that the spin structure can be tailored by judiciously choosing the geometry.

Introduction

Due to a number of interesting magnetic and electronic properties, such as high spin polarization, elevated Curie temperatures, shape memory effects, and high magneto-optical constants, Heusler compounds are a widely studied class of materials [1–8]. In particular, these materials are interesting for spintronic applications, where the combination of high spin polarization [3, 4], high Curie temperatures [9], and large values of the magnetization allow for a great variety of applications, such as spin polarized materials for applications as magnetic layers in magneto-resistance junctions [1, 10, 11], and also more complex devices such as artificial multiferroic systems based on magneto-electric coupling [12].

In order to use these interesting properties for applications within the field of spintronics, it is necessary to characterize the behavior of these materials in application relevant geometries. In particular, as the current lithographical technologies allow for the fabrication of nanoscale devices, the detailed characterization of the magnetic configuration of these materials at the nanoscale is a fundamental step towards applications.

Co_2MnGa (CMG) is a Co-based Heusler compound exhibiting a spin polarization of $P \simeq 0.55$ at room temperature [13], which can be epitaxially grown as thin films on different substrates such as GaAs [14] and MgO [13]. Due to the use of gallium in the Z site of the X_2YZ Heusler compound, CMG exhibits a higher oxidation resistance than other Co-based Heusler compounds with atoms such as Al or Si more prone to oxidation at the Z site [15]. In the work presented in this article, we analyze the influence of geometric confinements at the nanoscale on the magnetic configuration of CMG nanostructures by x-ray magnetic microscopy. We find that the magnetization configuration of nanostructured CMG elements is mainly determined by the contribution of shape anisotropy, thus rendering this material particularly interesting for applications, as its magnetic configuration can be reproducibly and reliably controlled solely by shape anisotropy, and thus by engineering the geometry of the single elements.

Experimental

Thin 30 nm thick films of CMG were fabricated from a commercial CMG target (Hauner Metallische Werkstoffe GmbH) by RF sputtering (Ar pressure of 0.1 mbar, with an applied RF power of 25 W, under the

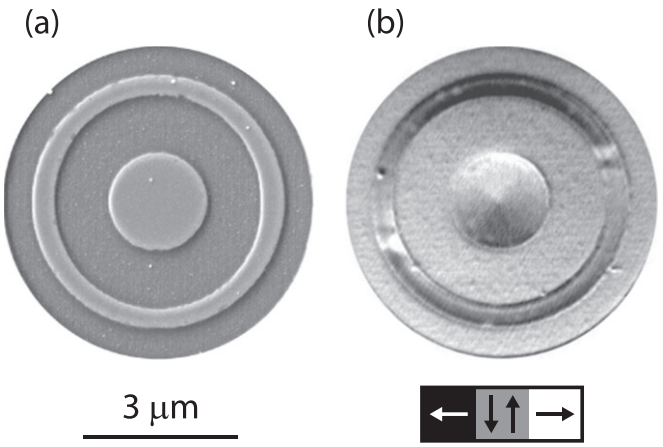

Figure 1. (a) Scanning electron micrograph of CMG ring and disk nanostructures fabricated by means of FIB lithography; (b) corresponding XMCD-PEEM image, exhibiting a clear magnetic contrast in the FIB lithographed nanostructures. A vortex state can be observed in the central disk, and a magnetic onion state can be observed in the outer CMG ring where two vortex domain walls have formed. The grayscale arrows indicate the direction of the magnetic contrast in (b).

same conditions as in [15]) on MgO (001) substrates (Crystec GmbH) at room temperature. As the MgO lattice constant is $a_{MgO} = 4.212$ Å, the [100] axis of the CMG crystal ($a_{CMG} = 5.77$ Å) grows parallel to the [110] direction of the MgO substrate (i.e. $\sqrt{2}\,a_{MgO} = 5.94$ Å). The as-deposited films were annealed at a temperature of 550 °C for 300 s, changing their crystalline order from the B2 to the $L2_1$ phase, as observed by *in-situ* reflection high-energy electron diffraction (RHEED) measurements [16] and *ex-situ* x-ray diffraction (XRD) scans (Bruker D8 Diffractometer) after the deposition. In order to prevent the oxidation of the CMG, a capping layer consisting of 3 nm of Al was sputter deposited on top of the CMG film. The capping layer was removed by Ar sputtering (available *in-situ* at the x-ray magnetic microscopy beamlines) prior to imaging by magnetic microscopy.

Magnetic hysteresis loops of the continuous CMG films were acquired by superconducting quantum interference measurements (SQUID, from Quantum Design), and by longitudinal magneto-optical Kerr effect (MOKE) measurements performed at room temperature employing a red ($\lambda = 635$ nm) low noise laser diode (Coherent).

Nanostructures of various sizes and geometries were fabricated from the CMG thin films by means of focused ion beam (FIB) lithography (FEI Helios NanoLab 600i), employing a 30 kV accelerated Ga^+ ion beam. As shown in figure 1(a), where a scanning electron micrograph of the CMG nanostructures fabricated by FIB lithography is shown, this technique allows for the fabrication of well-defined and magnetically decoupled structures, as shown in figure 1(b), where a magnetic image of the same nanostructures is shown. The fabrication of the nanostructures by FIB lithography did not induce any detectable damage in the capping layer on the nanostructures outside of the exposed regions.

The magnetic configuration of the nanostructured CMG has been imaged using photoemission electron microscopy (PEEM), exploiting the x-ray magnetic circular dichroism (XMCD) at the Co L_3 edge (about 780 eV) to obtain a magnetic contrast [16]. These measurements were carried out at the Nanospectroscopy beamline at Elettra [17] and at the CIRCE beamline at ALBA [18], both equipped with an Elmitec SPELEEM setup (type LEEM III). An *in-situ* electromagnet, integrated with the PEEM sample holder [19], was employed to apply a magnetic field to the nanostructures along the [110] direction of the CMG in order to manipulate their magnetic configuration. All the measurements have been carried out at room temperature and in the remnant state.

Results and discussion

As shown in figure 2(a), θ–2 θ XRD scans of the CMG films exhibit only (00*l*) reflections, and no secondary phases or orientations were observed. In figure 2(b), ϕ-scans carried out on the (111) reflections of the CMG demonstrate the presence of a clear four-fold symmetry with $L2_1$ order induced by high temperature annealing [16]. Furthermore, by comparing the respective peak positions of the CMG films and the MgO substrate as shown in figure 2(b), a 45° in-plane rotation of the CMG unit cell with respect to that of the MgO substrate has been observed.

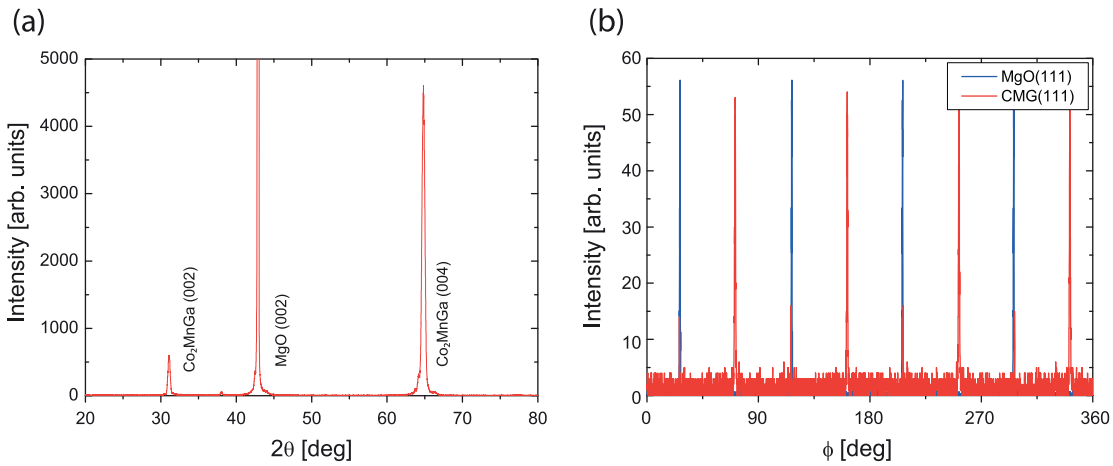

Figure 2. (a) θ—2θ XRD scan of a CMG sample with a thickness of 30 nm; (b) ϕ-scan of the same sample carried out at the (111) and equivalent peaks of the CMG (red curve). Additionally, the (111) and equivalent peaks of the MgO substrate (blue curve) are shown.

The CMG films analyzed in this work exhibit a saturation magnetization M_s of about 3.2 μ_B per formula unit at 5 K (determined by SQUID magnetometry) [15]. The M_s reduces by 6% at room temperature, indicating a Curie temperature well above 300 K. As shown in figure 3, from angle-resolved longitudinal MOKE measurements of the CMG films it was possible to identify a four-fold magnetic anisotropy, with the easy axes along the ⟨110⟩ crystallographic directions.

To determine the magnitude of the four-fold anisotropy constant K_1 of the CMG thin films, we employed the Stoner–Wohlfarth formalism [20], describing the magnetization of the CMG as a single rotating *macro-spin*, and expressing the magnetic free energy density as follows [20]:

$$F = -\mu_0 H M_s \cos(\theta) + K_1 \sin^2(\theta - \phi)\cos^2(\theta - \phi), \quad (1)$$

with θ being the angle between the magnetization vector **M** of the material and the applied magnetic field vector **H**, and ϕ the angle between the easy axis of the four-fold anisotropy term and the applied magnetic field vector **H**. As can be observed in (1), the Stoner–Wohlfarth model does not include the magnetic free energy terms that describe the contribution of the formation of magnetic domains. However, for the reversible part of the hysteresis loops (i.e. when relaxing the external magnetic field from the saturation value H_s to zero), in particular along directions close to the hard-axes, the Stoner–Wohlfarth model constitutes a reasonable approximation for the behavior of the thin film magnetization [7, 21].

We calculated the minimum of the magnetic free energy density given in (1), obtaining a function $\theta = \theta(H)|_{K_1}$ and fitted it to the reversible part of the hysteresis loops of the CMG measured by MOKE magnetometry, with K_1 as the fitting parameter. As shown in figure 4, where a fit for the reversible part of the CMG hysteresis loop for an angle $\phi = 30°$ is shown, it is possible to obtain a reasonable fit for a value of the four-fold anisotropy constant of $K_1 = 1500 \pm 150\ \mathrm{J\,m^{-3}}$, which is comparable to other Co-based Heusler compound thin films [1].

Also, in agreement with the behavior of other Co-based Heusler compound thin films [8, 22], the coercive field of the CMG thin films exhibits a maximum along the ⟨100⟩ directions and rapidly decreases at neighboring angles, as shown in figure 3. This behavior was interpreted as being due either to the formation of a checkerboard domain pattern at the switching of the magnetization [8], or as being due to magnetic frustration effects during the reversal process [22]. It was not possible to verify the microscopic origin of this increase in the coercive field for the analyzed CMG thin films, as XMCD-PEEM imaging can be carried out only close to the magnetic remnant state.

After having determined the main properties of the continuous CMG films, we now turn our attention to the analysis of the influence of geometric confinement on the magnetic domain structure of the CMG. The magnetic configuration of the nanostructured CMG elements, determined by XMCD-PEEM imaging, is compared with micromagnetic simulations, carried out by numerical time integration of the Landau–Lifshitz–Gilbert equation with a finite-difference method. The calculations were performed with the help of the MicroMagnum framework [23], using a value of $A = 4 \times 10^{-11}\ \mathrm{J\,m^{-1}}$ for the exchange stiffness, and the values of the saturation magnetization and magneto-crystalline anisotropy given above. These values lead to an exchange length of ca. 13 nm, and thus a numerical discretization with a cell of $x \times y = 5 \times 5\ \mathrm{nm^2}$ was used. The value of the exchange length was estimated by carrying out a simulation of the same structure (in this particular case, of a nanostructured CMG square with 1 μm × 1 μm edges along the ⟨110⟩ crystalline directions of the CMG) with

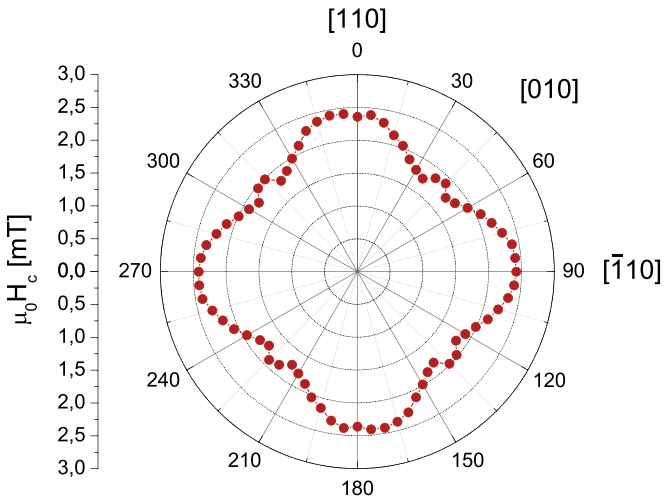

Figure 3. MOKE magnetometry measurements of a 30 nm thick CMG sample, showing the angular dependence of the coercive field H_c. It is possible to observe that the CMG exhibits a four-fold magnetic anisotropy, with the easy axis along the ⟨110⟩ directions, and the hard axis along the ⟨100⟩ directions. The points from 180° to 360° have been mirrored from the measured points from 0° to 180°.

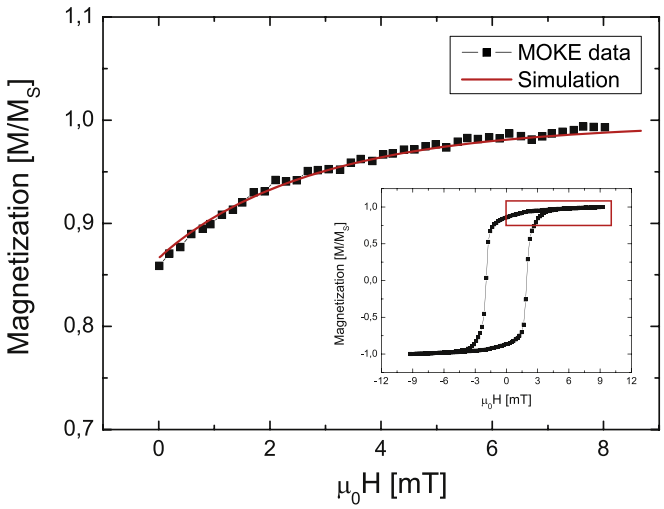

Figure 4. Reversible part of the hysteresis loop for a 30 nm thick CMG thin film sample measured with MOKE at an angle of 30° with respect to the [110] crystallographic direction of the CMG (black squares). The red curve shows the reversible part of the hysteresis loop calculated using the Stoner–Wohlfarth model assuming a four-fold anisotropy constant of $K_1 \approx 1.5\ \mathrm{kJ\,m^{-3}}$. The value of the magnetization pointing along the applied magnetic field has been normalized to the saturation magnetization. The full hysteresis loop is shown in the inset, with the part fitted with the Stoner–Wohlfarth model marked in red.

different values of the exchange stiffness, and comparing the simulated state with the experimentally determined magnetic configuration.

In figure 5(a), a series of images acquired at the remnant state (after the application of a magnetic field of ca. 50 mT along the [1 $\bar{1}$ 0] direction of the CMG) of nanostructured squares of different sizes and orientations is presented. In particular, the squares were oriented with their edges either along the ⟨100⟩ or the ⟨110⟩ directions of the CMG. As can be observed in figure 5(a), the preferred magnetic domain configuration is the flux-closure Landau state [24] for both orientations of the square edges for square edges of 2 μm and below. However, as can be observed in figure 5(a), for larger squares (i.e. an edge size of 4 μm and above) the contribution of the magneto-crystalline anisotropy term can be observed: if the edges of the square nanostructure are pointing along the ⟨110⟩ crystallographic directions of the CMG, it is possible to observe an undistorted Landau flux-closure state also for the larger squares. Instead, if the edges of the nanostructured square are pointing along the ⟨100⟩ directions, a deformed Landau flux-closure state can be observed. These results are in agreement, as shown in figure 5(b), with the micromagnetic simulations.

As shown in figure 6, where the micromagnetic simulations of the nanostructured squares with a 4 μm edge size are presented, the effect of the different orientation of the square edges with respect to the magneto-

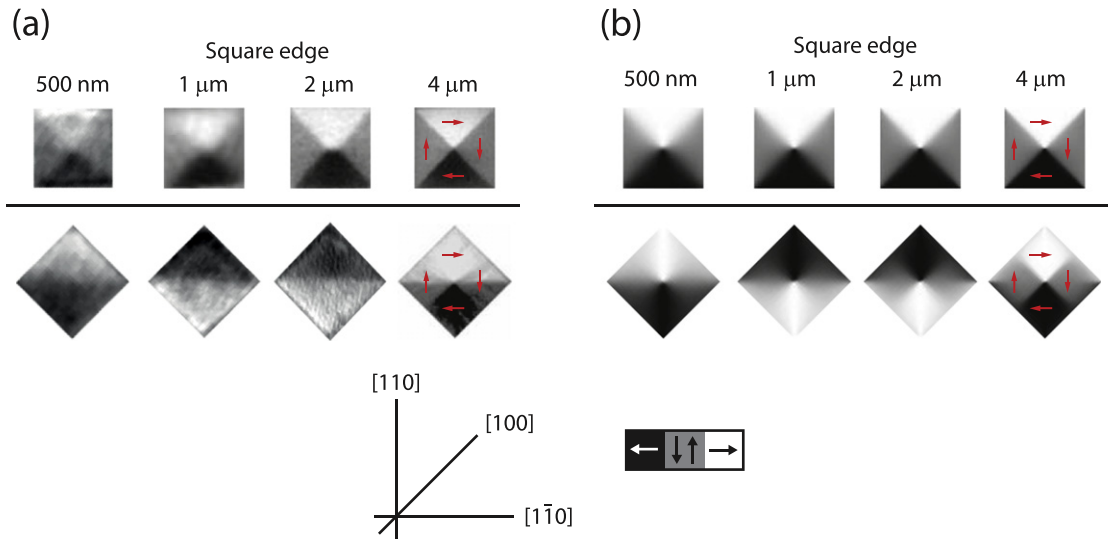

Figure 5. XMCD-PEEM images (a) and corresponding micromagnetic simulations (b) of the nanostructured CMG squares of different geometrical dimensions and orientations with respect to the CMG crystallographic axes (the dimension of the edge of the single square elements is indicated on the top of the image). The preferred magnetic state is given by the Landau flux-closure state. As confirmed by the micromagnetic simulations, if the edges of the nanostructured squares are pointing along the ⟨110⟩ crystallographic directions of the CMG, a clear Landau flux-closure state is stabilized independently of the size of the nanostructure. Instead, if the edges of the nanostructured squares are pointing along the ⟨100⟩ directions, a distortion of the Landau flux-closure pattern can be observed both in the images and in the corresponding simulations, due to the interplay between the shape and magneto-crystalline anisotropy contributions. The grayscale arrows indicate the direction of the magnetic contrast in the images, and the red arrows in the 4 μm wide square nanostructures indicate the direction of the magnetization in the single domains.

crystalline anisotropy leads to a different magnetic configuration. In particular, when the contributions of the shape and magneto-crystalline anisotropy terms are competing with each other (i.e. if the edges of the square are pointing along the ⟨100⟩ directions of the CMG), a flux-closure pattern with a distinctly different magnetic configuration compared to the Landau flux-closure state (4 μm bottom squares in figure 5) is visible. The comparison shown in figure 6 makes these differences easily visible. Thus, by selecting the geometry and orientation of the nanostructured CMG squares, it is possible to achieve control of the width of the domain walls of the Landau flux-closure pattern.

Furthermore, circular nanostructured elements with different diameters were analyzed both with XMCD-PEEM imaging and by determining their magnetic configuration with the help of micromagnetic simulations. As shown in figures 7(a) and (b), both the XMCD-PEEM imaging and the micromagnetic simulations reveal that the favored magnetic state for the nanostructured elements is the vortex state. These results show that by fabricating circular nanostructures it is possible to reliably stabilize the vortex domain configuration independently (at least, for the analyzed dimensions, which are of relevance for spintronic applications) from the diameter of the nanostructured element.

Finally, to study the spin structure of magnetic domain walls in the CMG, which is of critical importance for numerous spintronic applications such as for example current induced domain wall motion, ring-shaped nanostructures were analyzed, as shown in figure 8. After the initialization with a magnetic field along the [1 $\bar{1}$ 0] direction, the rings were predominantly in the onion state [25], exhibiting both a head-to-head and a tail-to-tail domain wall, with predominantly vortex-type wall configurations [26]. In contrast, for wide rings with a high local curvature, such as the 1 μm wide ring with a diameter of 2 μm shown in figure 8, the flux closure state seems to be energetically favored. Micromagnetic simulations of the nanostructured rings were also carried out. However, in this case, the favored magnetic configuration is the magnetic onion state with transverse wall configurations [26]. The reason behind this discrepancy between the simulated and experimentally determined magnetic configurations could be the different temperatures at which the two analyses were carried out: the micromagnetic simulations were carried out at an effective temperature of 0 K, while the XMCD-PEEM imaging experiments were carried out at room temperature. Such differences in the temperature can lead to the stabilization of a different magnetic domain wall configuration, as observed e.g. for $La_{0.7}Sr_{0.3}MnO_3$ nanostructured half-ring elements [27].

We thus find that the magnetic configuration of small CMG nanostructures is largely determined by the shape-anisotropy for the geometries analyzed in the work presented here. From the results of the micromagnetic simulations, it is possible to observe that, for the square nanostructures with their edges oriented along the ⟨100⟩

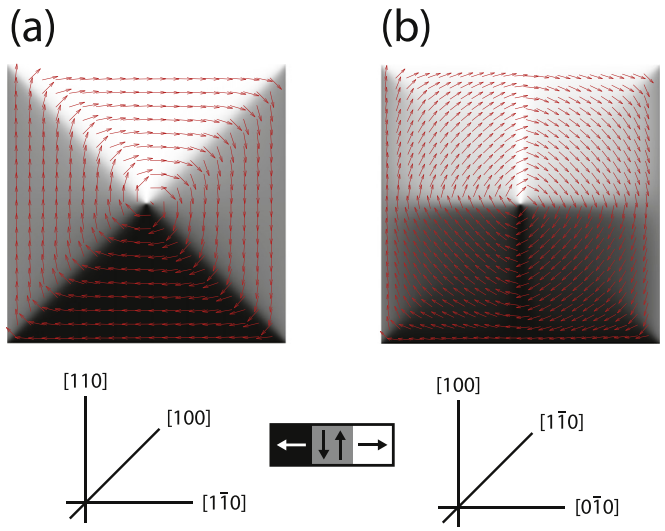

Figure 6. Micromagnetic simulations of a 4 μm wide CMG square with its edges oriented along (a) the ⟨110⟩ directions of the CMG (i.e. the easy axes of the magneto-crystalline anisotropy) and along (b) the ⟨100⟩ directions of the CMG (i.e. the hard axes). A clear influence of the orientation of the nanostructured squares on their magnetic configuration can be observed, demonstrating that for this (and larger) geometries, shape anisotropy is not the only dominant contribution to the magnetic configuration. The red arrows visualize the direction of the local magnetization in the two nanostructures.

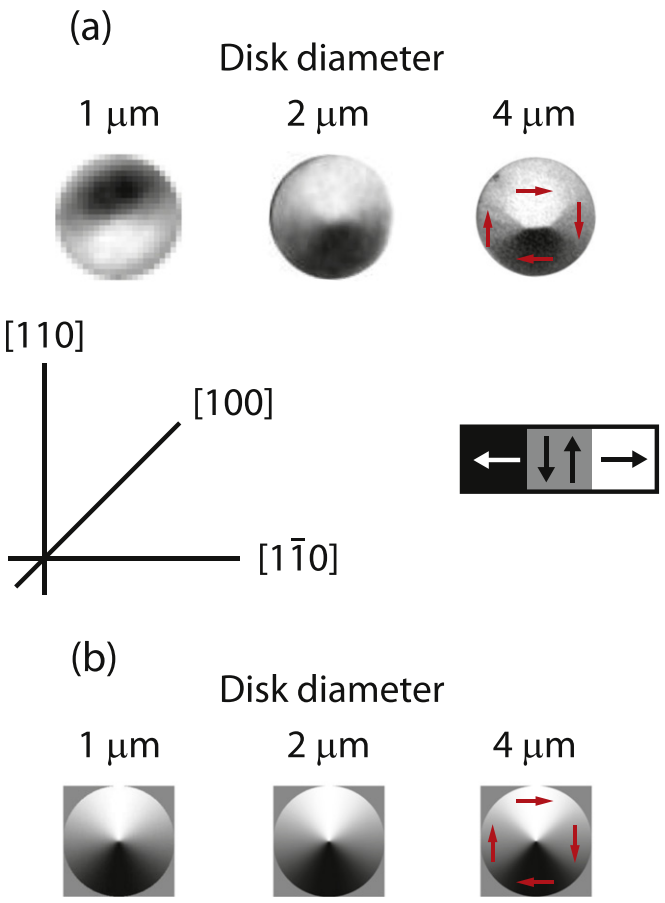

Figure 7. XMCD-PEEM images (a) and corresponding micromagnetic simulations (b) of CMG circular nanostructures of different diameters (indicated at the top of the image). For all the observed disk diameters, the preferred magnetic state is a vortex state (the direction of rotation is opposite for the 1 μm disk as compared to the 2 and 4 μm disks), as also confirmed by micro-magnetic simulations. The grayscale arrows indicate the direction of the magnetic contrast in the images, and the red arrows in the 4 μm diameter disk nanostructures indicate the direction of the magnetization in the four domains (four-quadrant state which the magnetic configuration evolves into for larger disks).

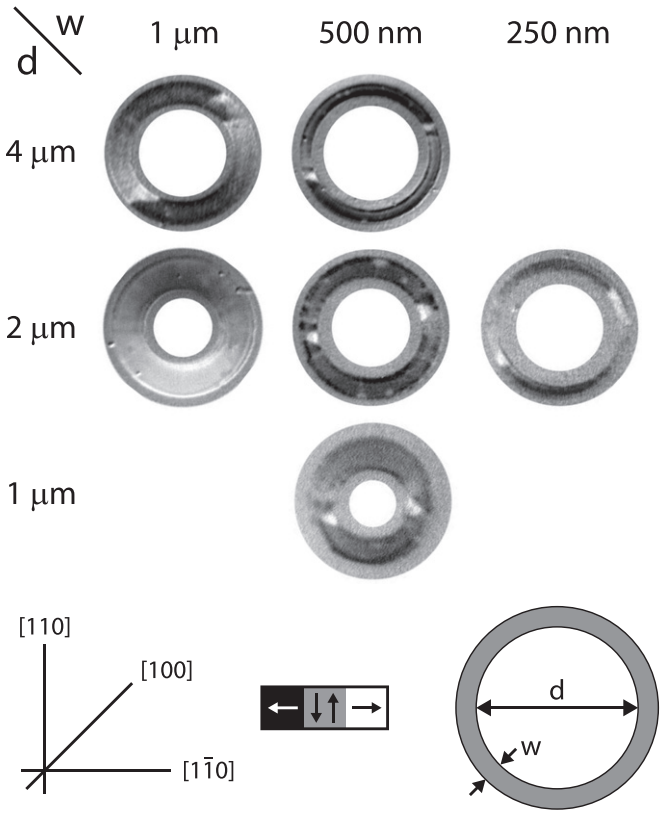

Figure 8. XMCD-PEEM images of nanostructured CMG rings of different diameters d and widths w. The preferred domain wall structure is given by a vortex wall, while for a high ring curvature (i.e. $w = 1\ \mu$m, and $d = 2\ \mu$m), the ring exhibits a single magnetic flux-closure domain. No preferential orientation with respect to the crystallographic axes of the CMG for the magnetic domain walls has been observed. The grayscale arrows indicate the direction of the magnetic contrast in the images.

crystalline directions of the CMG (i.e. the hard axes of the cubic anisotropy), that the contributions of the shape and magneto-crystalline anisotropies become comparable for squares with an edge of ca. 4 μm and, for these and dimensions above these, the magnetic configuration is no longer dominated by the sole contribution of shape anisotropy.

Conclusions

In conclusion, the magnetic configurations of the FIB-nanostructured CMG Heusler compound have been characterized by means of XMCD-PEEM imaging. The films were heteroepitaxially grown on MgO (001) substrates by RF sputtering, and exhibit an $L2_1$ order after suitable annealing, as confirmed by XRD and RHEED measurements. MOKE measurements allowed us to observe that the CMG thin films in the $L2_1$ order exhibits a four-fold symmetry for the magnetic easy axes, which lay along the $\langle 110 \rangle$ crystalline directions of the CMG. The magnitude of the cubic anisotropy term was estimated to be $K_1 = 1500 \pm 150\ \mathrm{J\,m^{-3}}$. As observed in XMCD-PEEM imaging and confirmed by micromagnetic simulations, the magnetic configuration of the CMG nanostructures is governed, for dimensions below ca. 4 μm, by shape anisotropy, thus allowing for the control of the magnetic configuration in the patterned CMG elements, making this material a good candidate for spintronic applications. The results reported in this paper focus on the analysis of the magnetic configurations of nanostructured CMG elements resulting from the combined (magnetic) contributions of the Co and Mn atoms. A possible future study could be the analysis of the atomic magnetic moments arising from the Co and Mn atoms in the CMG, which would also allow for the comparison of the effect of different growth conditions (e.g. with CMG films grown on GaAs substrates [28]) on the magnetic properties of this material.

Acknowledgments

Part of this work was carried out at the Nanospectroscopy beamline of the Elettra synchrotron light source, Basovizza (TS), Italy and at the CIRCE beamline of the ALBA Synchrotron Light Facility, Cerdanyola del Valles,

Spain. For their contribution to the CIRCE beamline the authors thank J Nicolás, E Pellegrin, S Ferrer, V Pérez-Dieste and C Escudero. The authors thank G Herranz and B Casals (ICMAB, Spain) for their help with the MOKE measurements. The authors further acknowledge the financial support from the EU 7th Framework Programme IFOX (Grant No. NMP3-LA-2010 246102), MAGWIRE (Grant No. FP7-ICT-2009–5 257707), CALIPSO (Grant No. FP7/2007–2013 312284), the European Research Council through the Starting Independent Researcher Grant MASPIC (Grant No. ERC-2007-StG 208162), the Graduate School of Excellence 'Materials Science in Mainz' (Grant No. GSC 266), and the Deutsche Forschungsgemeinschaft (DFG) through the SpinCat project (Grant No. KL 1811/7-1).

References

[1] Trudel S, Gaier O, Hamrle J and Hillebrands B 2010 *J. Phys. D: Appl. Phys.* **43** 193001
[2] Takanashi K 2010 *Japan. J. Appl. Phys.* **49** 110001
[3] Jourdan M *et al* 2014 *Nat. Commun.* **5** 3974
[4] Marukame T, Ishikawa T, Hakamata S, Matsuda K-I, Uemura T and Yamamoto M 2007 *Appl. Phys. Lett.* **90** 012508
[5] Graf T, Felser C and Parkin S 2011 *Prog. Solid State Chem.* **39** 1
[6] Vaz C *et al* 2011 *Appl. Phys. Lett.* **99** 182510
[7] Miyawaki T *et al* 2013 *J. Appl. Phys.* **114** 073905
[8] Gaier O, Hamrle J, Hermsdoerfer S, Schultheiß H, Hillebrands B, Sakuraba Y, Oogane M and Ando Y 2008 *J. Appl. Phys.* **103** 103910
[9] Webster P 1971 *J. Phys. Chem. Solids* **32** 1221
[10] Sakuraba Y, Hattori M, Oogane M, Ando Y, Kato H, Sakuma A, Miyazaki T and Kubota H 2006 *Appl. Phys. Lett.* **88** 192508
[11] Chen L, Chen C, Jin K and Du X 2012 *Europhys. Lett.* **99** 57008
[12] Yamauchi K, Sanyal B and Picozzi S 2007 *Appl. Phys. Lett.* **91** 062506
[13] Kolbe M, Chadov S, Jorge E A, Schönhense G, Felser C, Elmers H-J, Kläui M and Jourdan M 2012 *Phys. Rev.* B **86** 024422
[14] Holmes S N and Pepper M 2002 *Appl. Phys. Lett.* **81** 1651
[15] Hahn M, Schönhense G, Jorge E A and Jourdan M 2011a *Appl. Phys. Lett.* **98** 232503
[16] Stöhr J, Wu Y, Hermsmeier B, Samant M, Harp G, Koranda S, Dunham D and Tonner B 1993 *Science* **259** 658
[17] Locatelli A, Cherifi S, Heun S, Marsi M, Ono K, Pavlovska A and Bauer E 2002 *Surf. Rev. Lett.* **9** 171
[18] Aballe L, Foerster M, Pellegrin E, Nicolas J and Ferrer S 2015 *J. Synchrotron Radiat.* **22** 745
[19] Heyne L, Kläui M, Rhensius J, le Guyader L and Nolting F 2010 *Rev. Sci. Instrum.* **81** 113707
[20] Stoner E and Wohlfarth E 1948 *Phil. Trans. R. Soc.* A **240** 599
[21] Gabor M, Petrisor T Jr, Tiusan C, Hehn M and Petrisor T 2011 *Phys. Rev.* B **84** 134413
[22] Ruiz-Calaforra A, Conca A, Graf T, Casper F, Leven B, Felser C and Hillebrands B 2013 *J. Phys. D: Appl. Phys.* **46** 475001
[23] MicroMagnum (http://micromagnum.informatik.uni-hamburg.de)
[24] Hubert A and Schäfer R 1998 *Magnetic Domains: The Analysis of Magnetic Microstructures* (Berlin: Springer-Verlag)
[25] Rothman J, Kläui M, Lopez-Diaz L, Vaz C, Bleloch A, Bland J, Cui Z and Speaks R 2001 *Phys. Rev. Lett.* **86** 1098
[26] Kläui M 2008 *J. Phys.: Condens. Matter* **20** 313001
[27] Finizio S *et al* 2014 *J. Phys.: Condens. Matter* **26** 456003
[28] Claydon J, Hassan S, Damsgaard C, Bindslev Hansen J, Jacobsen C, Xu Y and van der Laan G 2007 *J. Appl. Phys.* **101** 09J506